

1 Article

# 2 The Distal and Local Volcanic Ash in the Late 3 Pleistocene Sediments of the Termination I Interval at 4 the Reykjanes Ridge, North Atlantic, Based on Study 5 of the Core AMK-340

6 Alexander Matul <sup>1,\*</sup>, Irina F. Gablina <sup>2</sup>, Tatyana A. Khusid <sup>1</sup>, Natalya V. Libina <sup>1</sup>, and Antonina I.  
7 Mikhailova <sup>2</sup>

8 <sup>1</sup> Shirshov Institute of Oceanology, Russian Academy of Sciences, Nahimovskiy prospekt 36, 117997  
9 Moscow, Russia; AM: amatul@mail.ru, TAK: tkhusid@mail.ru, NVL: lnatvit@mail.ru

10 <sup>2</sup> Geological Institute, Russian Academy of Sciences, Pyzhevskii per. 7, 119107 Moscow, Russia; IFG:  
11 igabl@rambler.ru, AIM: amikhailova-07@mail.ru

12

13 \* Correspondence:

14 Alexander Matul, Shirshov Institute of Oceanology, Nahimovskiy prospekt 36, 117997 Moscow, Russia;

15 E-mail: amatul@mail.ru; Tel. +7-499-1292172

16 **Abstract:** Based on the geochemical analysis of the volcanic material from the sediment core  
17 AMK-340, central zone of the Reykjanes Ridge, we could detect two ash-bearing sediment units  
18 accumulated during the Termination I. They correlate to the Ash Zone I in the North Atlantic Late  
19 Quaternary sediments having an age of 12170-12840, within the Younger Dryas cold chronozone,  
20 and 13600-14540 years, within and Bølling-Allerød warm chronozone. The ash of the Younger  
21 Dryas unit is presented mostly by the mafic and persilicic material originated from the Icelandic  
22 volcanoes; Vedde Ash is presented in one sediment sample from this unit. The ash of the  
23 Bølling-Allerød unit is presented mostly by the mafic shards which are related to the basalts of the  
24 rift zone on the Reykjanes Ridge, having presumably the local origin. A detection of Vedde Ash  
25 helped to specify the timing of the previously reconstructed paleoceanographic changes for the  
26 Termination I in the point of study: a significant warming in the area could occur as early as 300  
27 years prior to the end of the conventional Younger Dryas cold chronozone.

28 **Keywords:** tephra in marine sediments; Ash Zone I in North Atlantic; tephrochronology of  
29 Termination I

30

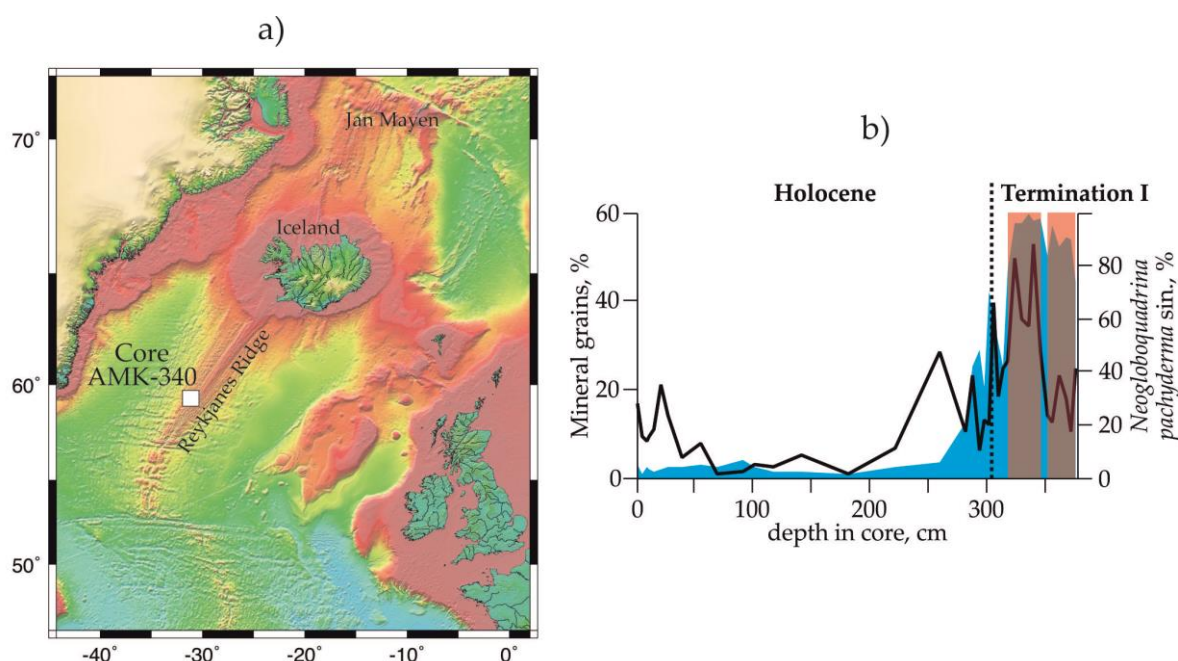
## 31 1. Introduction

32 Tephrochronology is a widely used tool for dating and correlating of the marine and terrestrial  
33 sediment sequences, especially within the Quaternary [1]. Recent detailed mineralogical and  
34 geochemical studies of the volcanic material revealed a high-resolution Late Pleistocene and  
35 Holocene chronostratigraphy for the North Atlantic [2-4]. Icelandic volcanoes are the major source of  
36 the ash in the marine sediments of the Nordic Seas and North Atlantic [5]. Extensive studies of the  
37 Icelandic soil, lake and shelf sediments documented >150 tephra layers formed during the  
38 Termination I and Holocene [6]. Thornalley et al. [7] detected numerous ash-bearing marine  
39 sediment layers south of Iceland within the last deglacial and Holocene time. Such data help to  
40 refine the regional and local sediment stratigraphy, and synchronize the paleoclimatic archives  
41 between the distal oceanic and land regions.

42 The aim of our study is to get an additional information on the occurrence and composition of  
 43 the tephra in the North Atlantic sediments at the transition from the last glacial to the Holocene. The  
 44 sediment core AMK-340 is situated in the central zone of the Reykjanes Ridge where an eruptive  
 45 material is produced. Therefore, we try to recognize the different sources of the volcanic ash, local or  
 46 distal ones. A geochemical analysis of the volcanic shards using the scanning electron microscopy  
 47 will help to reveal the specific well-known tephra layers like the Vedde Ash which can be used for a  
 48 refinement of the core stratigraphy and chronology of the local paleoceanographic changes.

## 49 2. Materials and Methods

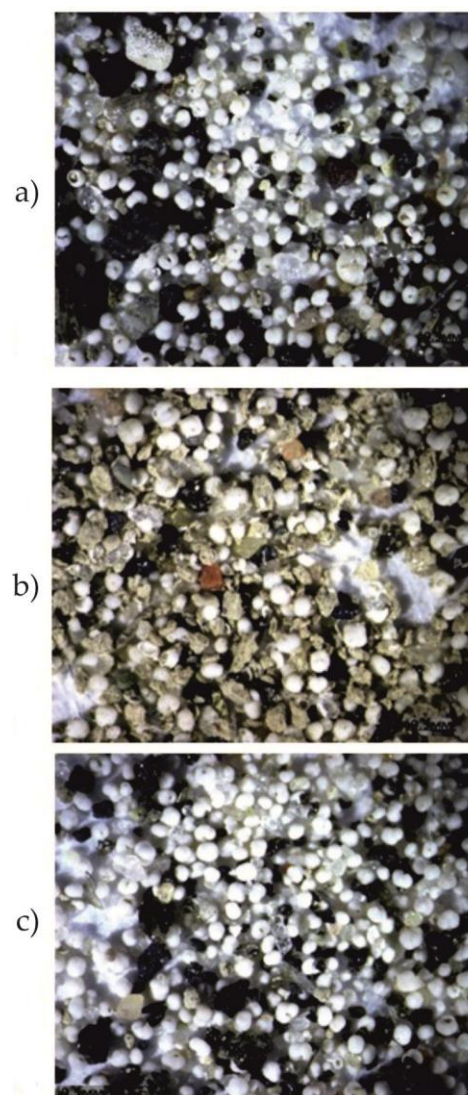
50 The sediment core AMK-340 was obtained during the 4<sup>th</sup> cruise of the Russian RV “Akademik  
 51 Mstislav Keldysh” [8] in the central part of the Reykjanes Ridge, North Atlantic south of Iceland (Fig.  
 52 1a): 58°30.6′ N, 31°31.2′ W, water depth of 1689 m, core length 387 cm. The core unit of 0-307 cm is  
 53 composed of the white pelitic calcareous or weakly calcareous (foraminiferal-coccolith) oozes with a  
 54 CaCO<sub>3</sub> content from 10-25 to 40-50%. In the lower core unit of 307-387 cm, a sediment color becomes  
 55 mainly grey with thin alternation of greenish-grey, yellowish-grey, and dark almost black bands.  
 56 This unit is enriched in the diatoms (sometimes up to 10-30%), the CaCO<sub>3</sub> content varies there  
 57 between 5.5 and 20% [8]. A visual lithological description of the core exhibited no signs of the  
 58 volcanic material.



59  
 60 **Figure 1.** Sediment core AMK-340: a) geographic position (source of map is <[https://topex.ucsd.edu/marine\\_topo/jpg\\_images/topo4.jpg](https://topex.ucsd.edu/marine_topo/jpg_images/topo4.jpg)>), b) position of the ash-bearing units within the core,  
 61 blue-colored graph is a distribution of the polar planktic foraminifera *Neogloboquadrina*  
 62 *pachyderma sinistral* [9] as glacial marker, black line is a distribution of the mineral grains in the  
 63 sediment fraction of >100 μm [9] as a marker of the ice-rafted material, red bars are the ash-bearing  
 64 core units.  
 65

66 During the micropaleontological foraminiferal analysis of the core AMK-340 sediments under  
 67 the stereomicroscope (Fig. 2), we could recognize a remarkable admixture of the eruptive shards in  
 68 the sediment fraction of >100 μm from two core units (Fig. 1b), 323-340 cm (four samples 323-325,

69 328-330, 334-336, and 338-340 cm) and 355-378 cm (four samples 355-357, 360-368, 370-372, and  
70 376-378 cm). We analyzed those samples where a content of the eruptive material was >10-15% from  
71 the whole number of grains in the sediment fraction of >100  $\mu\text{m}$ . The eruptive shards from every  
72 sample for the following studies of their chemical composition were picked out. All in all, 24 shards  
73 in the natural state, 25 shards from the core unit of 323-340 cm and 16 shards from the core unit of  
74 355-378 cm in the polished thin sections were analyzed. The chemical composition of the shards was  
75 examined (1) by a scanning electron microscope CamScan MV2300 with energy dispersive analysis  
76 system INCA in the Geological Institute of the Russian Academy of Sciences, Moscow, Russia,  
77 (shards in the natural state), and (2) by the scanning electron microscope VEGA3 TESCAN with  
78 energy dispersive analysis system INCA in the Institute of Oceanology of the Russian Academy of  
79 Sciences, Moscow, Russia, (shards in the polished thin sections). The regular microphotographs of  
80 the sediment fractions were made on the stereomicroscope ZEISS Stemi 508 equipped by the camera  
81 AxioCam Icc5.



82

83 **Figure 2.** Microphotographs of the sediment fraction >0.1 mm: a) core sample of 323-325 cm, b)

84 sample of 328-330 cm, c) sample of 338-340 cm.

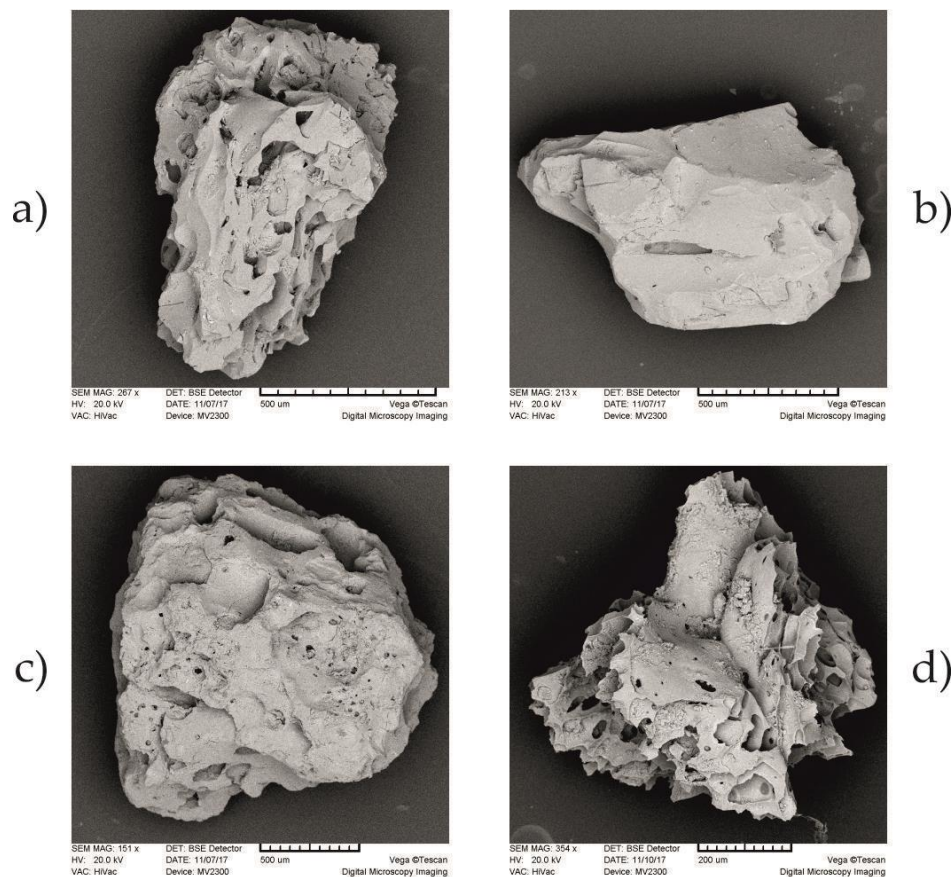
85 An age model of the core AMK-340 was developed on the linear interpolation between four AMS  
86  $^{14}\text{C}$ -datings [9] taking into account five old conventional  $^{14}\text{C}$ -datings [10-11]. The core spans time

87 interval of the last appr. 14500 years or the Termination I and Holocene. A possible detection of the  
 88 Vedde Ash with the age of 12170 years [3, 12-13] in the sample 323-325 cm (see Discussion section)  
 89 allows us to make more accurate age model of the sediment core AMK-340 for the time interval of  
 90 the Termination I (sharp warming with the climatic fluctuations between the Last Glacial Maximum  
 91 and Holocene). From new calculations regarding the Vedde Ash detection, the lower time limit of  
 92 the core AMK-340 is 14540 years B.P. The core units of 323-340 and 355-378 cm can have the age of  
 93 12170-12840 and 13600-14540 years, respectively.

### 94 3. Results

#### 95 3.1. Morphological types of the eruptive material in the studied sediment samples

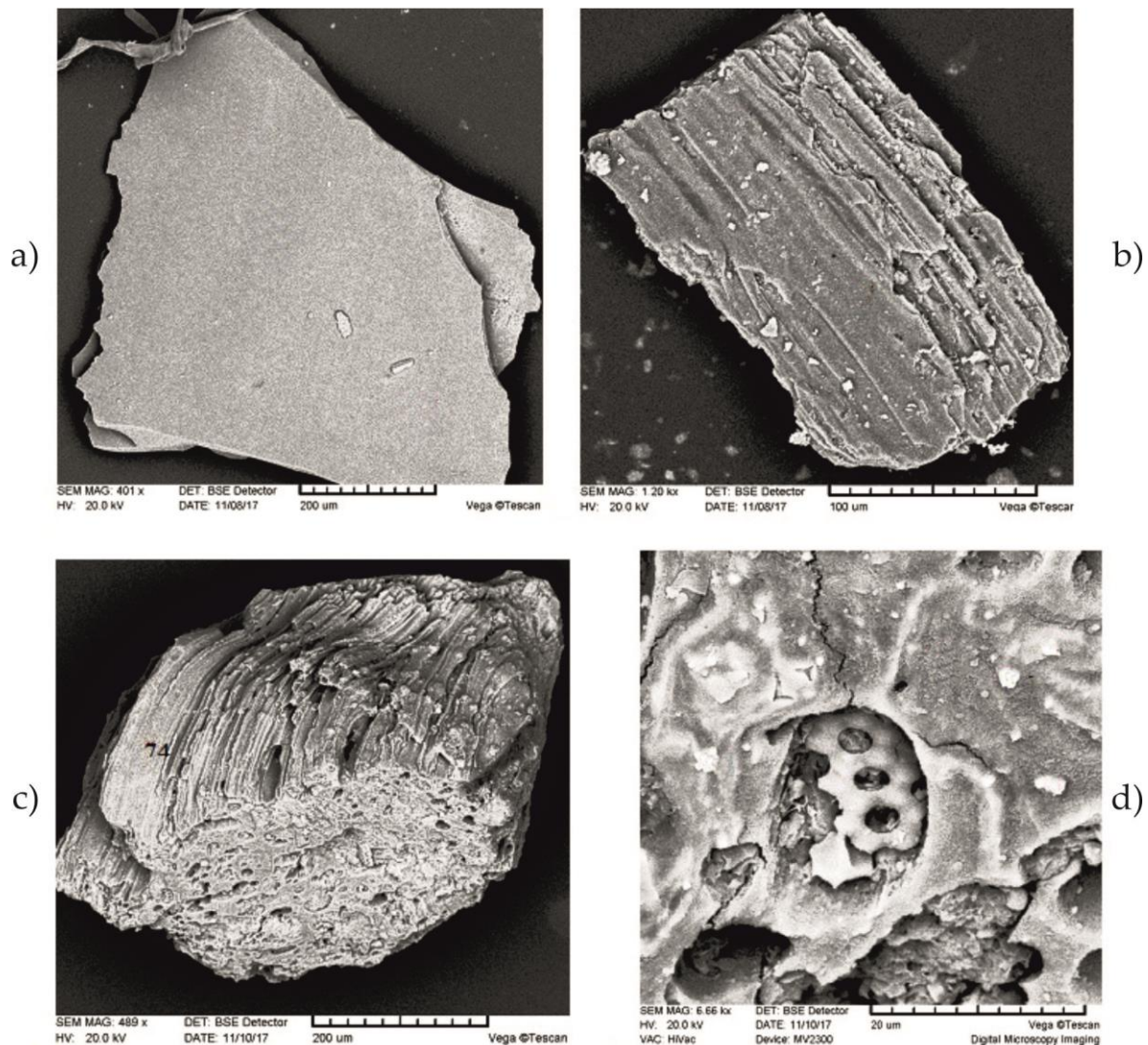
96 Angular fragments of the pumiceous basalts and basaltic andesites, black and sometimes  
 97 greenish, aphanitic (microlitic) and porous, with cavities filled by the light volcanic ash and  
 98 sometimes by the fragmented diatom frustules (Fig. 3).



99

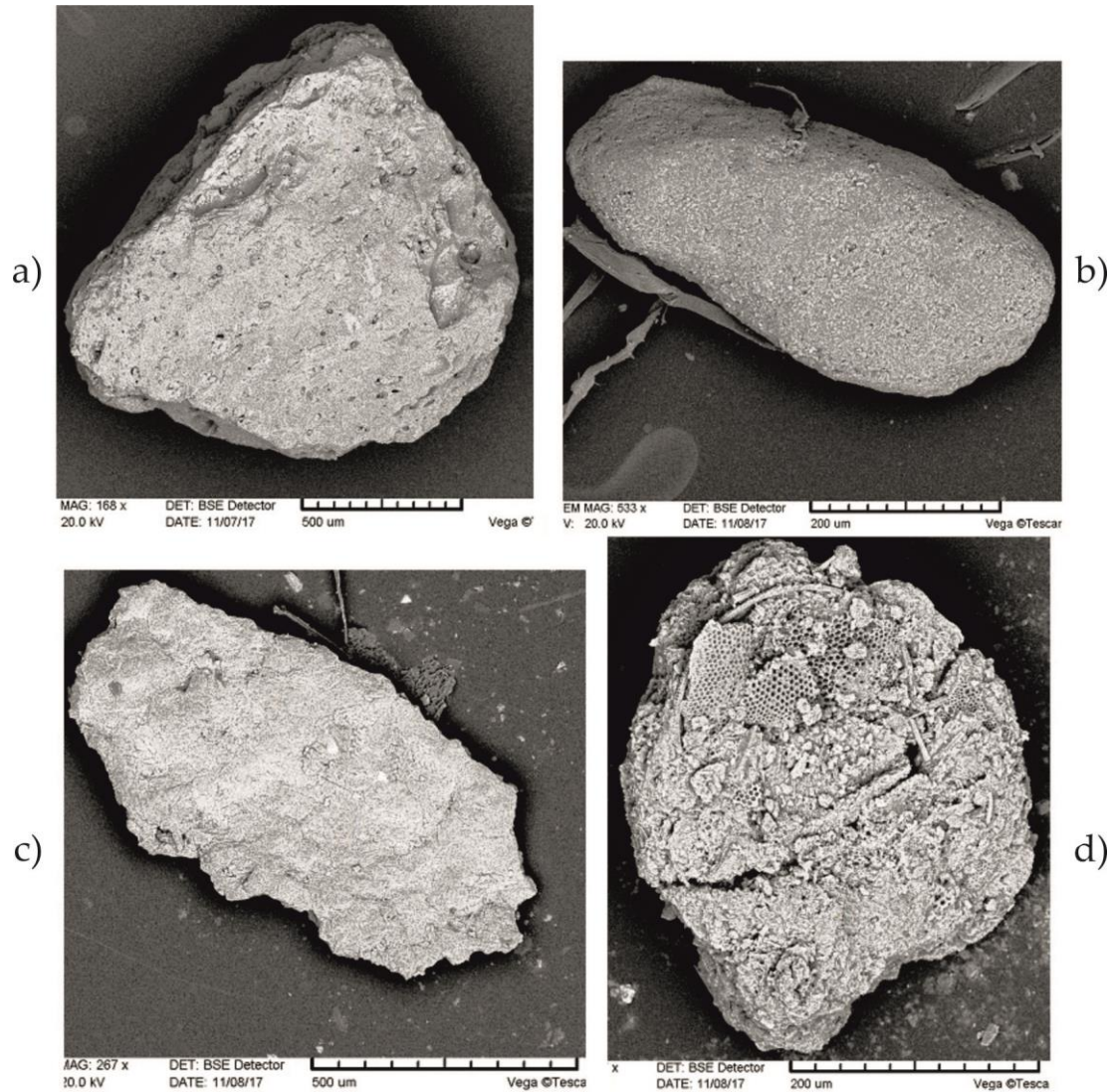
100 **Figure 3.** Scanning electron microphotographs of the basalt and andesitic basalt ash shards from  
 101 the core unit of 323-340 cm: a) vesicular black basalt glass with SiO<sub>2</sub> of 49.10 to 57.15% in the  
 102 sample of 323-325 cm, b) massive black semi-transparent glass with SiO<sub>2</sub> of 49.45% in the sample of  
 103 323-325 cm, c) vesicular black shard (SiO<sub>2</sub> of 50.22%) with cavities filled by the andesitic (SiO<sub>2</sub> of  
 104 55.79%) and persilicic (SiO<sub>2</sub> of 63.89-65.97%) dust in the sample of 323-325 cm, d) highly vesicular  
 105 dark-green semi-transparent andesitic basalt glass with SiO<sub>2</sub> of 52.52% in the sample of 334-336  
 106 cm.

107 Angular transparent/subtransparent fragments of the persilicic glass, olive and bottle-green,  
 108 elongate (columnar) with rough scratching on the surface parallel to the elongation, or having an  
 109 irregular shape, aphanitic (Fig. 4).



110  
 111 **Figure 4.** Scanning electron microphotographs of the persilicic ash shards from the core unit of  
 112 323–340 cm: a) angular dense greenish transparent glass with a median content of SiO<sub>2</sub> of 76.37% in  
 113 the sample of 323–325 cm, b) rectangular light semi-transparent dense foliated shard with SiO<sub>2</sub> of  
 114 75.57–76.88% in the sample of 328–3330 cm, c) and d) general view and fragment, respectively, of  
 115 vesicular greenish semi-transparent glass (SiO<sub>2</sub> of 70.38%) in the sample of 334–336 cm, with  
 116 layered andesitic insertions (SiO<sub>2</sub> of 55.90%) and titanomagnetite crystals and fragments of diatom  
 117 frustules.

118 Pisolites as rounded/semi-rounded grains and fragmentary grains, light (almost white),  
 119 massive and occasionally porous, composed of the persilicic and andesitic ash with inclusions of the  
 120 fragmented diatom frustules, titanomagnetite and quartz (Fig. 5b-d).



121

122

123

124

125

126

127

128

129

**Figure 5.** Scanning electron microphotographs of the andesitic ash shards and pisolites from the core unit of 323-340 cm: a) rounded fine-pored black heterogeneous andesitic shard with SiO<sub>2</sub> of 53.30-53.66% in the sample of 323-325 cm, the sheet-like fragments with higher SiO<sub>2</sub> of 55.50-56.05% and small ilmenite crystals are included, b) light pisolite composed of the andesitic basalt ash dust with SiO<sub>2</sub> of 62.03-65.98% in the sample of 323-325 cm, small titanomagnetite crystals are included, c) light loose grain composed of the andesitic basalt ash dust in the sample of 328-330 cm, small ilmenite and titanomagnetite crystals are included, d) white pisolite composed of the diatom frustules fragments and volcanic dust in the sample of 328-330 cm.

130

Pisolites as semi-rounded/non-rounded grains, black, composed of the andesitic and mafic ash with inclusions of the fragmented diatom frustules, quartz and pyroxene (Fig. 5 and 6a-b, 6d).

131

In addition, mostly rounded, transparent, colorless sometimes rose or yellow-brown (ferruginized) quartz.

132

What are pisolites in our samples?

133

134

Part of the ash material is the rounded and semi-rounded aggregates of the very thin, usually slightly cemented ash particles in size of  $\leq 50 \mu\text{m}$  having the various composition with a sometimes substantial admixture of the fragmented diatom frustules, sponge spicules and other microfossils.

135

136

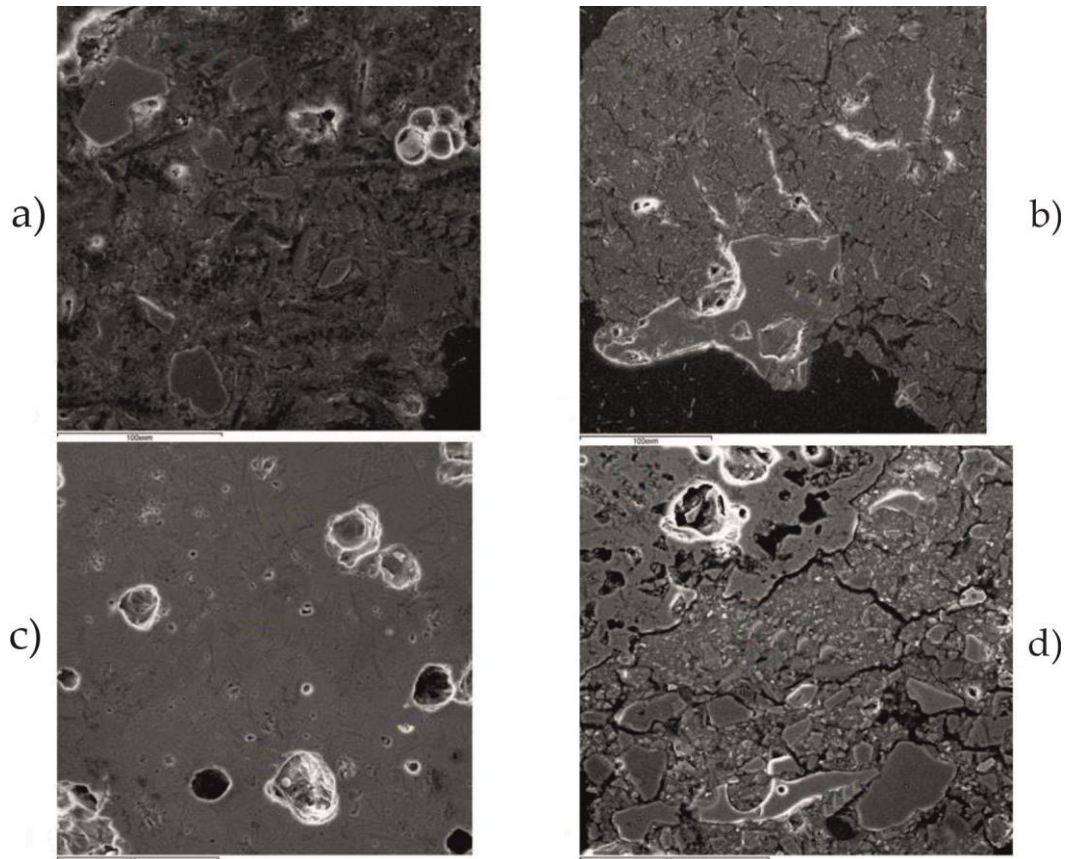
We assign them as pisolites or ash shatters. They are aggregates of thin volcanic ash which can be

137

138

139 formed during the penetration of the rain drops within the ash clouds, also during the vapor  
 140 condensation on the ash particles in the eruptive clouds [14-17]. According the classification of the  
 141 volcanoclastic material in [18], particles <0.1 mm are the fine-grained ash dust. This material appears  
 142 at the andesite volcanic eruptions, and an area of its dispersal is unlimited. It can be contaminated by  
 143 the terrestrial particles (e.g., minerals, fresh-water diatoms) during the eolian transport and by the  
 144 marine particles (e.g., microfossils) during the sedimentation in the ocean.

145 We could recognize two types of pisolites in our samples: 1) semi-rounded, black, dense,  
 146 sometimes pumiceous aggregates of the mixed composition, and 2) rounded, white, loose  
 147 aggregates of the intermediate composition (Fig. 5 and 6).



148  
 149 **Figure 6.** Scanning electron microphotographs of the basalts and pisolites of the andesitic and mafic  
 150 composition on the polished thin sections from the core unit of 323-340 cm: a) irregularly elongated  
 151 non-rounded black grain composed of mainly andesitic ( $\text{SiO}_2$  of 52.39-58.97%) and sometimes  
 152 persilicic ( $\text{SiO}_2$  of 64.94%) dust in the sample of 328-330 cm, larger mafic shards, quartz and  
 153 microfossil fragments are included, b) semi-rounded black shard composed of the andesitic ash dust  
 154 with  $\text{SiO}_2$  in the mean of 57.5% in the sample of 328-330 cm, occasional larger basalt shards with  $\text{SiO}_2$   
 155 of 49.22% are included, c) microlitic basalt glass with  $\text{SiO}_2$  in the mean of 50.31% in the sample of  
 156 328-330 cm, microlites are intermediate/mafic plagioclase, d) semi-rounded black shard composed of  
 157 the andesitic ash dust with  $\text{SiO}_2$  of 54.83% in the sample of 338-340 cm, occasional larger basalt  
 158 fragments with  $\text{SiO}_2$  in the mean of 50.52% and some Fe oxides (?) are included.

159

### 160 3.2. Distribution of the eruptive material in the studied sediment samples

#### 161 3.1.1. Core unit of 323-340 cm with an age of 12170-12840 years

162 We found here the abundant ash particles and pisolites, together with the foraminiferal shells, from  
163 0.1-0.5 to 2-2.5 mm sometimes up to 6.5 mm in size (Fig. 2). Black fragments (basalts,  
164 andesito-basalts, pisolites of the intermediate and mafic composition) prevail in the upper and lower  
165 parts of the unit, samples of 323-325 and 334-336 cm, respectively, with a content of 30-40% of the  
166 whole sediment fraction (Fig. 2). The largest fragments of >1.5 mm in size are typical for the upper  
167 part of the unit.

168 The content and size of the black eruptive fragments decrease sharply in the sample of 328-330 cm;  
169 they comprise 5-10% of the sediment fraction, and their size normally is <0.5-1 mm. In this sample,  
170 the light pisolites of 0.25-0.5 mm in size, composed of the persilicic and andesitic ash with quartz, do  
171 prevail reaching 50-70% of the sediment fraction.

172 The content of the volcanic particles in the lowermost part of the unit, sample 338-340 cm, decreases  
173 significantly down to 8-10% of the sediment fraction. They are presented mostly by the black  
174 volcanic glass with an admixture of the olive-green ash, white pisolites of the persilicic composition,  
175 quartz, rare fragments of the pyroxene and plagioclase. Size of the particles rarely exceeds 1 mm  
176 with a maximum up to 2.5 mm.

#### 177 3.1.2. Core unit of 355-378 cm with an age of 13600-14540 years

178 The eruptive material is presented by the sharply angular mainly pumiceous black basalt fragments  
179 with a white ash dust in the cavities, the semi-transparent bottle-green, sometimes yellowish mafic  
180 glass particles, quartz, feldspar, and sporadic semi-rounded white pisolites composed of the  
181 persilicic and andesitic ash dust (Fig. 7). In the analyzed sediment fraction, fragments of the eruptive  
182 rocks and minerals are larger compared to the biogenic particles being of 0.5-1 mm, occasionally 2-4  
183 mm in size. The eruptive material within the unit is distributed irregularly with highest amounts up  
184 to 20-25% of the sediment fraction in the middle (sample 360-362 cm) and lower (sample 376-378 cm)  
185 parts; its content in other samples stands at 5-10%.

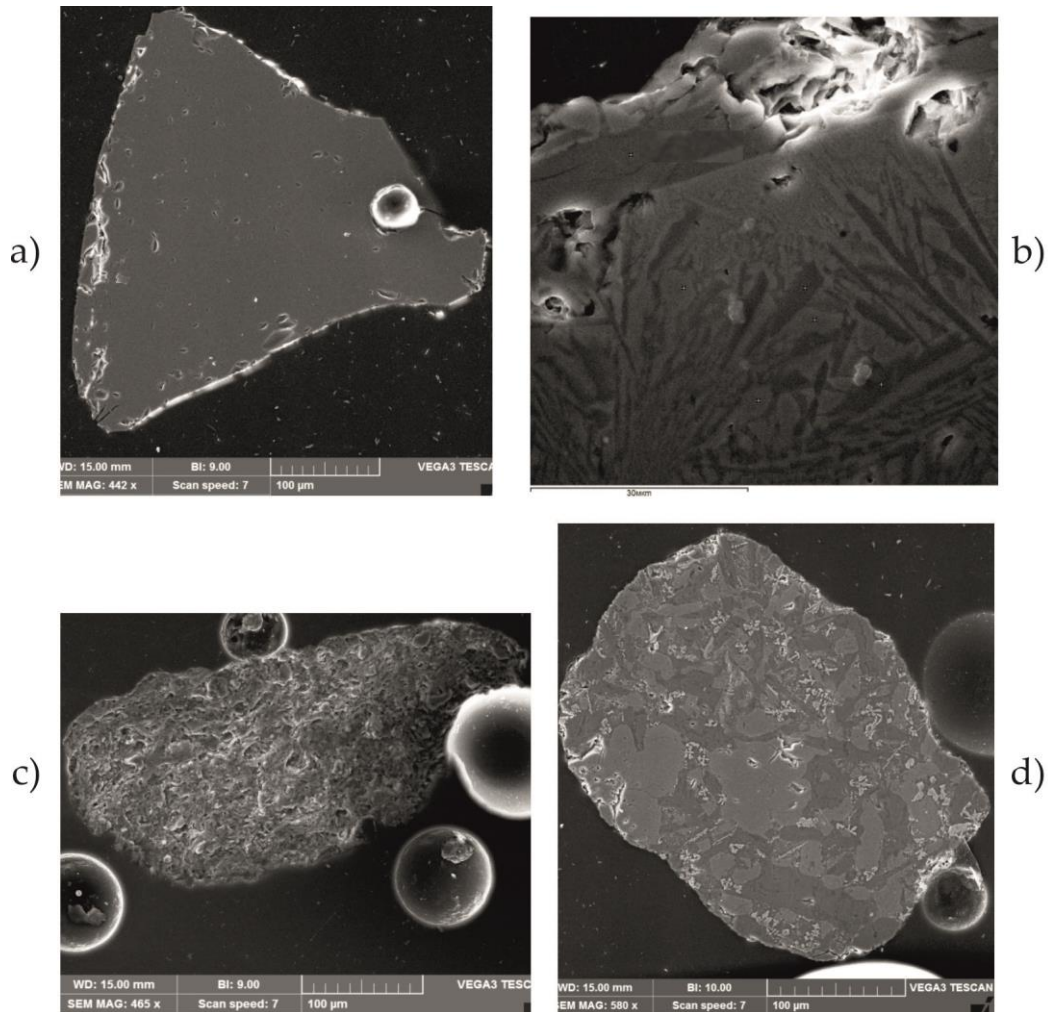
### 186 3.2. Chemical composition of the volcanic material in the studied samples

#### 187 3.2.1. Core unit of 323-340 cm with an age of 12170-12840 years

##### 188 3.2.1.1. Sample 323-325 cm

189 Basalt fragments, which prevail here, have typical content of SiO<sub>2</sub> from 49.05 to 51.67%,  
190 degraded concentration of K<sub>2</sub>O from 0 to 0.91%, and high TiO<sub>2</sub> amount from 1.49% to 5.43%. TiO<sub>2</sub>  
191 content drops down to 0.68% in some grains with highest SiO<sub>2</sub> concentration. Glass composition on  
192 the surface of one shard can vary in some cases from basaltic with SiO<sub>2</sub> of 49.10% to andesitic with  
193 SiO<sub>2</sub> of 57.15% (Fig. 3a). Cavities of the black pumiceous basalt fragments are filled in many cases by  
194 the volcanic ash dust of the different composition, from the andesitic one with SiO<sub>2</sub> of 55.79% to  
195 persilicic one with SiO<sub>2</sub> of 63.89% and 65.97% (Fig. 3c).

196 Rhyolites (volcanic persilicic shards) are less numerous than the basaltic fragments. We  
197 analyzed a chemical composition of one grain (Fig.4a) where SiO<sub>2</sub> and K<sub>2</sub>O content is high up to  
198 76.37% and 3.92%, respectively. TiO<sub>2</sub> is not found.



199

200

201

202

203

204

205

206

**Figure 7.** Scanning electron microphotographs of the eruptive shards on the polished thin sections from the core unit of 355–378 cm: a) andesitic basalt shard with SiO<sub>2</sub> of 52.60% in the sample of 355–357 cm, b) microlitic andesitic basalt glass shard with SiO<sub>2</sub> of 51.68% in the sample of 366–368 cm, intermediate/mafic crystals of plagioclase are included, c) persilicic pisolite with SiO<sub>2</sub> of 79.1% in the sample of 370–372 cm, some plagioclase (?) crystals are included, d) dark-grey andesitic pisolite with SiO<sub>2</sub> of 53.38–56.96% in the sample of 376–378 cm, light-grey basalt fragments (SiO<sub>2</sub> of 50.42–51.81%) are included.

207

208

209

210

Pisolites, which are presented here mostly by the white rounded loose intermediate variety (Fig. 5 and 6), are composed of the ash dust with SiO<sub>2</sub> content from 53.30–53.66 to 58.18% with occasional inclusions of the titanomagnetite. Black pisolites have fragments of the mixed mafic (SiO<sub>2</sub> of 42.08–50.76%) to persilicic (SiO<sub>2</sub> of 65.49% in average) composition.

211

### 3.2.1.2. Sample 328–330 cm

212

213

214

215

216

217

Most part of the volcanic material is presented by pisolites predominantly of the intermediate-persilicic composition (Fig. 5c–d) similar to those in the sample 323–325 cm. Ash dust in pisolites has SiO<sub>2</sub> content of 62.03–65.98%. Inclusions in pisolites are small crystals of titanomagnetite and ilmenite, and diatom frustules (Fig. 5d).

We found also pisolites of the mixed composition with the andesitic (SiO<sub>2</sub> of 58.97%) and persilicic (SiO<sub>2</sub> of 64.94%) ash dust, larger andesitic basalt particles (SiO<sub>2</sub> in the mean of 52.39%),

218 occasional quartz inclusions and high admixture of the microfossil fragments (mostly diatoms) (Fig.  
219 6a). Most black pisolites consist of the intermediate ash dust with SiO<sub>2</sub> in the mean of 57.5% and  
220 occasional larger basalt particles (Fig. 6b) with SiO<sub>2</sub> of 49.22%.

221 In addition, there are sporadic mafic with SiO<sub>2</sub> of 52.04%, intermediate with SiO<sub>2</sub> of 61.22%, and  
222 persilicic ash shards, the latter with high concentration of SiO<sub>2</sub> and K<sub>2</sub>O, of 75.11% in average and up  
223 to 4.88%, respectively. Some mafic shards are microlithic (Fig. 6c) and consist of the basalt glass with  
224 SiO<sub>2</sub> in the mean of 50.31% and thin mafic plagioclase microliths.

#### 225 3.2.1.3. Sample 334-336 cm

226 Eruptive material consists predominantly by the ash shards of the mafic (Fig. 3d) with SiO<sub>2</sub> of  
227 50-51%, persilicic with SiO<sub>2</sub> of 70.49-75.26% and K<sub>2</sub>O up to 3.39%, and mixed (Fig. 4B, r) composition.  
228 Less often, the andesitic basalt shards with SiO<sub>2</sub> of 52.78% occur. The persilicic shards are notable  
229 here for their elongate shape, presence of the lengthwise scratching, dense texture. Basalt shards  
230 have irregular shape and are pumiceous (Fig. 3 and 4). Shards of the mixed composition are close to  
231 the persilicic ones in the shape; on their transverse shear surfaces, we could see many small round  
232 cavities (bubbles) filled by the fragmented diatom frustules (Fig. 4c-d).

233 Some pisolites, consisted of thin andesitic ash dust with SiO<sub>2</sub> of 59.94 % and abundant diatom  
234 fragments, were found.

#### 235 3.2.1.3. Sample 338-340 cm

236 Basalt shards with SiO<sub>2</sub> of 50.17-51.01%, low K<sub>2</sub>O content of <1%, and high TiO<sub>2</sub> concentration  
237 up to 4.44% prevail in the sample. Andesitic basalt shards with SiO<sub>2</sub> of 53.46%, and sharply angular  
238 transparent persilicic glass shards with SiO<sub>2</sub> of 71.45-71.84% are less numerous. The latter have  
239 relatively high K<sub>2</sub>O content of 3.31-3.48%.

240 Sporadic black semi-rounded grains of the isometric or oval form are pisolites consisted of the  
241 andesitic ash dust with SiO<sub>2</sub> of 52.56-56.30% and occasional larger basalt shards (Fig. 6d) with SiO<sub>2</sub> in  
242 the mean of 50.52%.

#### 243 3.2.1. Core unit of 355-378 cm with an age of 13600-14540 years (Fig. 7).

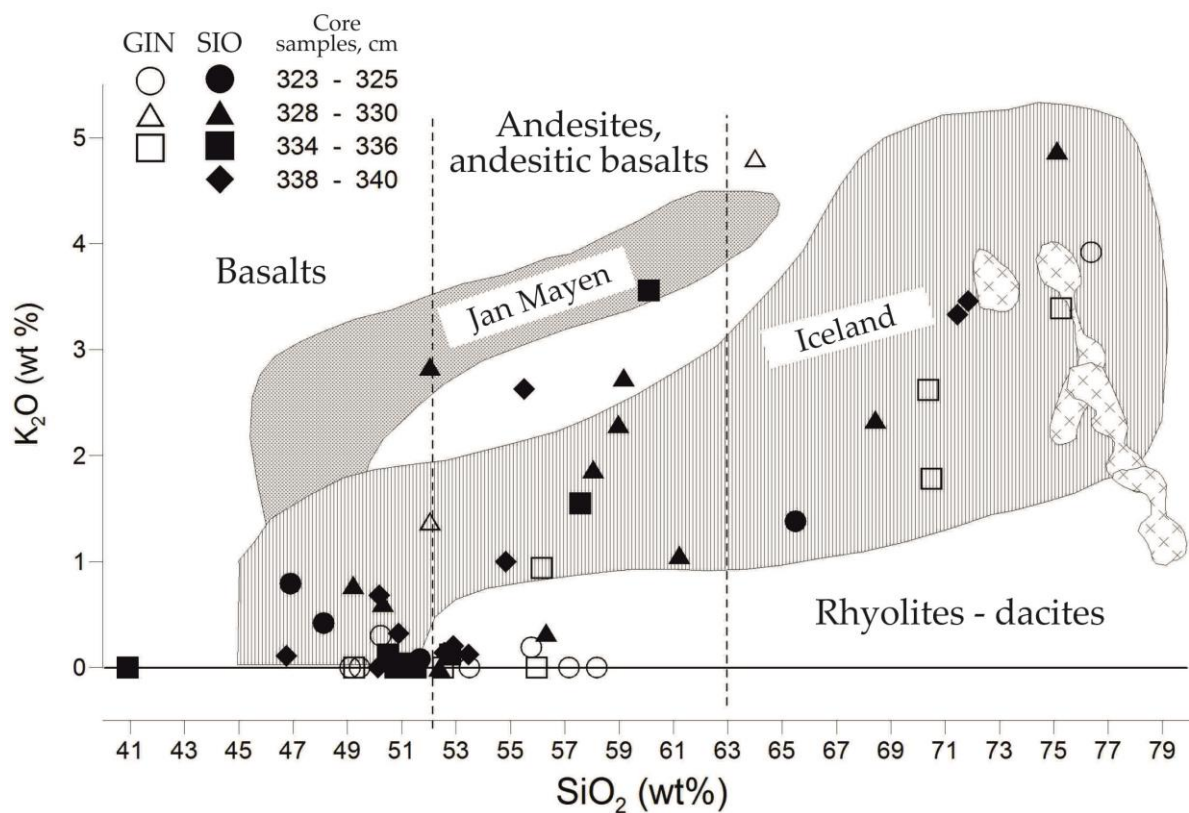
244 We analyzed 16 eruptive grains in the polished thin sections from 4 samples at 355-357, 360-368,  
245 370-372, and 376-378 cm. Most part of them is the andesitic basalt shards (Fig. 7a) with SiO<sub>2</sub> of 52.5%;  
246 they were found in all samples of this core unit. The sample 355-357 cm contains also andesitic  
247 volcanic shards with SiO<sub>2</sub> of 53.26 %, microlithic basalt shards with SiO<sub>2</sub> in the mean of 51.68% on  
248 three analyses, and intermediate-mafic plagioclase crystals (Fig. 7b). In the sample of 370-372 cm, we  
249 found the persilicic glass shard with SiO<sub>2</sub> of 66.90-67.65% and very high K<sub>2</sub>O concentration up to  
250 7.93%, and the persilicic pisolite (Fig. 7c) with SiO<sub>2</sub> of 79.1% and with intruded plagioclase. The  
251 sample 376-378 cm has the andesitic pisolites with SiO<sub>2</sub> of 53.38-56.96 % or in the mean of 55.17% and  
252 with intruded basalt fragments (SiO<sub>2</sub> of 50.42-51.81% or in the mean of 51.12%) and titanomagnetite  
253 (Fig. 7d), and basalt shards with SiO<sub>2</sub> of 45.88%.

## 254 4. Discussion

255 Mangerud et al. [19] and Kvamme et al. [20] summarized findings of the Vedde Ash, started as  
256 early as in 1940<sup>th</sup>, within the Younger Dryas chronozone sediments in the North Atlantic, Nordic  
257 Seas and surrounding European continental areas. Ruddiman and Glover [21] described a rhyolitic

258 ash bed in the pre-Holocene sediments from the North Atlantic which can be assigned as the  
 259 regional Ash Zone I. As the authors suggested, this ash bed must be mostly ice-rafted, and the ash  
 260 could be mixed through the sediment thickness of dozens of centimeters. In our core AMK-340 the  
 261 thickness of the ash-bearing sediments from two core units is 40 cm within the time interval of appr.  
 262 12100-14500 years B.P. Bond et al. [22] and Thornalley et al. [7], as earlier Kvamme et al. [20],  
 263 demonstrated a complicated geochemical composition of the ash beds in the Ash Zone I. The Vedde  
 264 Ash cannot be a simple synonym of the Ash Zone I. The latter contains the volcanic material  
 265 originated at different times from different Icelandic volcanoes and, probably, other sources. Based  
 266 on studies of our core, we can give more results on the differentiation of the ash within the Ash Zone  
 267 I in the open North Atlantic.

268 The diagram  $\text{SiO}_2$  versus  $\text{K}_2\text{O}$  on the Fig. 8 shows that most analyzed volcanic grains from the  
 269 core unit of 323-340 cm suit the ash material from the Icelandic volcanoes eruptions.



270  
 271  
 272  
 273

**Figure 8.** Position of the eruptive shards from the ash-bearing core unit of 325-340 cm in the binary  $\text{SiO}_2/\text{K}_2\text{O}$  system according [23]. Areas of the volcanic material from different sources are indicated according [24-25].

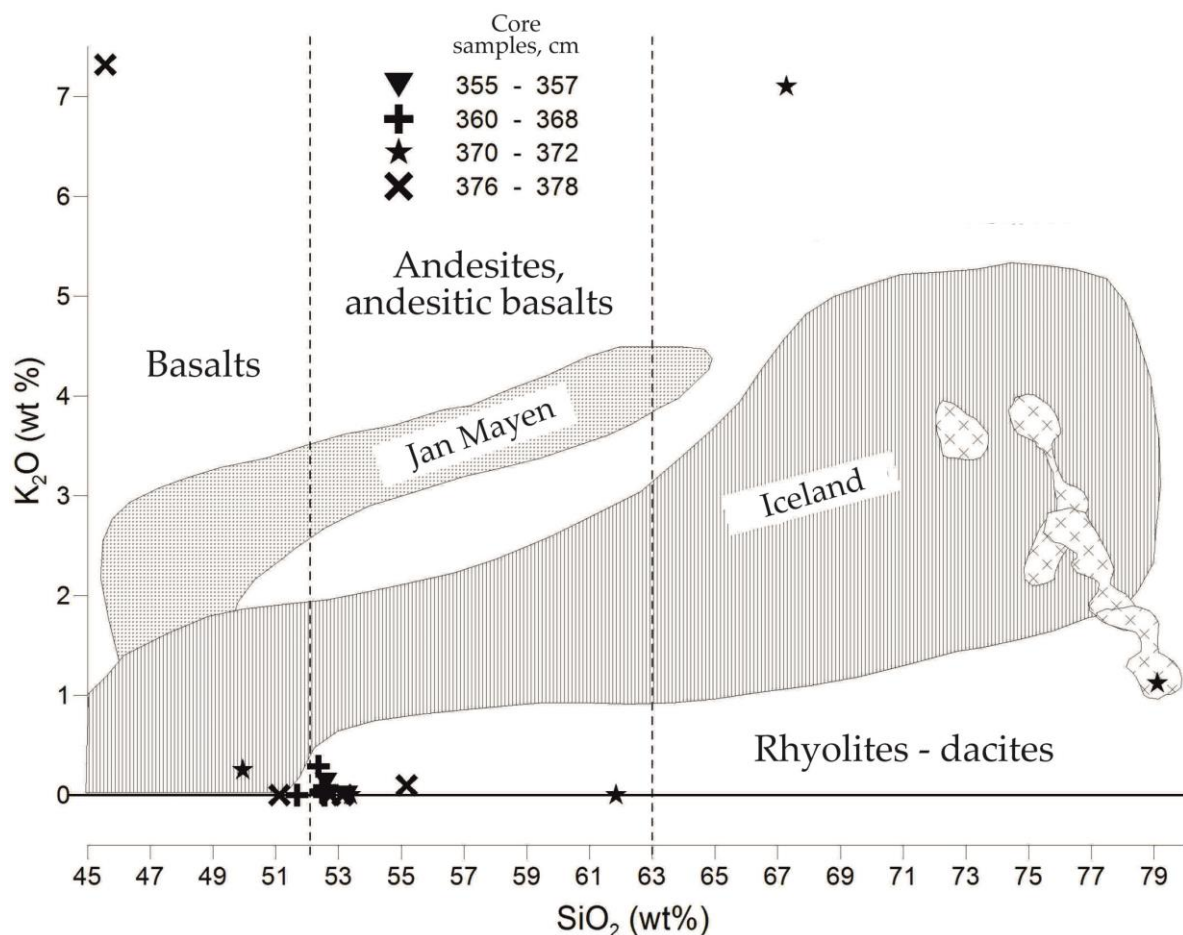
274 The sample of 323-325 cm contains the basalt shards and pisolites enriched in  $\text{TiO}_2$ , occasional  
 275 rhyolites with the elevated  $\text{K}_2\text{O}$  and high  $\text{FeO}$  concentrations. Such ash composition is typical for the  
 276 Vedde Ash whose age in the Greenland ice-core chronology appear to be  $12170 \pm 57$  years [3, 12-13]. A  
 277 source of the eruptive material for the Vedde Ash can be Katla volcano in the southern Iceland [20,  
 278 27]. In addition, we found some intermediate ash shards, also as dust in pisolites, with low  $\text{K}_2\text{O}$   
 279 content, but their origin is unclear.

280 In the core unit of 328-335 cm with the corrected age estimate of appr. 12700-12900 years, the  
 281 ash is presented mainly by the andesitic pisolites with the admixture of the basalts and rhyolites.  
 282 Most of them suit the material from the Icelandic volcanoes. But some basalt fragments with the  
 283 elevated  $\text{K}_2\text{O}$  in the andesitic pisolites can be related to the Jan Mayen volcanoes (Fig. 8). A common

284 occurrence of the marine microfossil (diatom) fragments inside pisolites and ash shard cavities may  
 285 suggest that the marine transportation and sedimentation could influence in a large degree an  
 286 accumulation of the volcanic material in the area of study. However, we cannot be sure of the Jan  
 287 Mayen origin of the above-mentioned andesitic pisolites because Abbot and Davies [3] noted that it  
 288 is rare to find the Jan Mayen volcanic deposits in the distal areas.

289 The ash in the core unit of 355-378 cm with an age of 13600-14540 years differs from that in the  
 290 core unit of 323-340 cm with an age of 12170-12840 years.

291 In the samples of 355-368 cm and 376-378 cm with an age of 13600-14100 and 14540 years,  
 292 respectively, we can see a dominance of the basalt and andesitic basalt shards with SiO<sub>2</sub> of  
 293 52.32-53.13%, FeO of 9.71-11.13%, MgO of 6.31-8.69%, and K<sub>2</sub>O of <1%. On the geochemical  
 294 composition they are close to the tholeiitic basalts and basalt glass in the rift zone of the Reykjanes  
 295 Ridge [8] (Fig. 9), but differ from them by higher SiO<sub>2</sub> concentration. SiO<sub>2</sub> content is 49.76% and  
 296 50.56% in average in the tholeiitic basalts and in the basalt shards of the Reykjanes Ridge,  
 297 respectively. It is possible that the ash in the core unit of 355-378 cm is mainly the local eruptive  
 298 material originated by the volcanism and tectonics in the Reykjanes Ridge rift zone [8], and  
 299 transformed under an influence of the acidic hydrothermal fluids during the sedimentation.



300  
 301  
 302  
 303

**Figure 9.** Position of the eruptive shards from the ash-bearing core unit of 355-378 cm in the binary SiO<sub>2</sub>/K<sub>2</sub>O system according [23]. Areas of the volcanic material from different sources are indicated according [24-25].

304 Other ash material in the core unit of 355-378 cm is (1) mafic shards with decreased SiO<sub>2</sub> of  
 305 45.88% in the lowermost sample of 376-378 cm, and (2) persilicic glass with SiO<sub>2</sub> of 67.65% and high  
 306 K<sub>2</sub>O concentration in the sample of 370-372 cm; source of both is unclear. Persilicic pisolites in the

307 sample of 370-372 cm and mafic pisolites with SiO<sub>2</sub> of 51.12% in the sample of 376-378 cm were  
308 possibly originated from the Icelandic volcanoes, but the source of the andesitic pisolites with SiO<sub>2</sub> of  
309 55.17% in the sample of 376-378 cm is not defined and could be more distal.

310 The Vedde Ash occurrence in the sediment sample of 323-325 cm made it possible to re-estimate  
311 the timing of the paleoenvironmental changes during the Younger Dryas chronozone (Glacial  
312 Stadial 1 in Rasmussen et al. [13]), which were reconstructed for the core AMK-340 [9]. Matul et al.  
313 [9] assigned the pre-Holocene warming at the Reykjanes Ridge in the North Atlantic within the  
314 Younger Dryas cold chronozone to the time interval of 12500-12200 years B.P. or significantly earlier  
315 than the beginning of the Holocene (11700 years B.P.). Now, we can assume that this change  
316 occurred 12200-12000 years B.P. which was anyways 300 years prior to the Holocene start.

## 317 5. Conclusions

318 Two sediment units of the core AMK-340, Reykjanes Ridge, North Atlantic, contain a significant  
319 amount of the volcanic ash. They can be related to the Ash Zone I in the North Atlantic Late  
320 Quaternary sediments. The ash-bearing sediments of the core were accumulated within the time  
321 intervals of 12170-12840 and 13600-14540 years B.P. or within the Younger Dryas cold chronozone  
322 and Bølling-Allerød warm chronozone, respectively.

323 The ash in the core AMK-340 within the Younger Dryas unit is presented mostly by the mafic  
324 and persilicic material originated from the Icelandic volcanoes, and ice-rafted to the point of study.  
325 In one sediment sample we could detect the bimodal Vedde Ash.

326 The ash in the core AMK-340 within the Bølling-Allerød unit is presented mostly by the mafic  
327 shards which are close to the basalts and basalt glass of the rift zone on the Reykjanes Ridge, i.e.,  
328 have presumably the local origin.

329 In some samples of both units we found pisolites aggregated of the andesitic ash dust with  
330 inclusions of the persilicic/mafic particles and fragments of the marine diatom frustules. An origin of  
331 these pisolites is unclear.

332 A detection of the Vedde Ash helped to specify the age model of the core AMK-340 for the  
333 Termination I time interval. Timing of the previously reconstructed paleoceanographic changes can  
334 be modified, but, anyways, a significant warming in the area could occur as early as 300 years prior  
335 to the end of the conventional Younger Dryas cold chronozone.

336 **Author Contributions:** Conceptualization, Alexander Matul; methodology, Irina F. Gablina; investigation, Irina  
337 F. Gablina, Tatyana A. Khusid, Antonina I. Mikhailova; writing—original draft preparation, Alexander Matul,  
338 Irina F. Gablina; writing—review and editing, Alexander Matul, Irina F. Gablina; visualization, Natalya V.  
339 Libina.

340 **Funding:** This research was funded by the Ministry of Education and Science of the Russian Federation, Project  
341 No. 0149-2019-0007 for the Shirshov Institute of Oceanology, and additional funding was from Project No.  
342 0135-2019-0050 for the Geological Institute (IFG and AIM).

343 **Acknowledgments:** Authors are grateful to N.V. Gorkova, V.V. Mikheev, A.G. Boev, G.Kh. Kazarina, and A.V.  
344 Tikhonova for valuable consultations and technical support.

345 **Conflicts of Interest:** The authors declare no conflict of interest. The funders had no role in the design of the  
346 study; in the collection, analyses, or interpretation of data; in the writing of the manuscript, or in the decision to  
347 publish the results.

## 348 References

- 349 1. Lowe, D.J. Tephrochronology and its application: a review. *Quat. Geochronol.* **2011**, *6*, 423.

- 350 2. Turney, S.M., Lowe, J.J., Davies, S.M., Hall, V.A., Lowe, D.J., Wastegård, S., Hoek, V.Z., Alloway, B.V.  
351 Tephrochronology of Last Termination sequences in Europe: a protocol for improved analytical  
352 precision and robust correlation procedures (a joint SCOTAV-INTIMATE proposal). *J. Quat. Sci.* **2004**,  
353 *21*, 335-345.
- 354 3. Abbott, P.M., Davies, S.M. Volcanism and the Greenland ice-cores: the tephra record. *Earth-Science Rev.*  
355 **2012**, *115*, 173-191.
- 356 4. Bourne, A.J., Cook, E., Abbot, P.M., Seierstad, I.K., Steffensen, J.P., Fischer, H., Schnupback, S., Davies,  
357 S.M. A tephra lattice for Greenland and a reconstruction of volcanic events spanning 25–45 ka b2k.  
358 *Quat. Sci. Rev.* **2015**, *118*, 122-141.
- 359 5. Thordarson, T., Höskuldsson, A. Postglacial volcanism in Iceland. *Jökull* **2008**, *58*, 198-228.
- 360 6. Gudmundsdóttir, E.R., Larsen, G., Björck, S., Ingólfsson, Ó., Striberger, J. A new high-resolution  
361 Holocene tephra stratigraphy in eastern Iceland: Improving the Icelandic and North Atlantic  
362 tephrochronology. *Quat. Sci. Rev.* **2016**, *150*, 234-249, <https://doi.org/10.1016/j.quascirev.2016.08.011>.
- 363 7. Thornalley, D.J.R., McCave, I.N., Elderfield, H. Tephra in deglacial ocean sediments south of Iceland:  
364 Stratigraphy, geochemistry and oceanic reservoir ages. *J. Quat. Sci.* **2011**, *26*, 190-198.
- 365 8. Lisitzin, A.P., Zonenshain, L.P., Eds. *Rift zone of the Reykjanes Ridge: tectonics, magmatism, conditions of*  
366 *sedimentation*. Nauka Press: Moscow, Russia, 1990; 239 pp. [In Russian].
- 367 9. Matul, A., Barash, M.S., Khusid, T.A., Behera, B., Tiwari, M. Paleoenvironment Variability during  
368 Termination I at the Reykjanes Ridge, North Atlantic. *Geosciences* **2018**, *8*, article 375. DOI:  
369 10.3390/geosciences8100375.
- 370 10. Matul, A. Late Quaternary paleoceanology of the North Atlantic based on radiolaria analysis data.  
371 *Oceanology* **1994**, *34*, 550-555.
- 372 11. Matul, A. On the problem of paleoceanological evolution of the Reykjanes ridge region (North  
373 Atlantic) during the last deglaciation based on a study of radiolaria. *Oceanology* **1994**, *34*, 806-814.
- 374 12. Mortensen, A.K., Bigler, M., Grönvold, K., Steffensen, J.P., Johnsen, S.J. Volcanic ash layers from the  
375 Last Glacial Termination in the NGRIP ice core. *J. Quat. Sci.* **2005**, *20*, 209-219.
- 376 13. Rasmussen, S.O., Bigler, M., Blockley, S.P., Blunier, T., Buchardt, S.L., Clausen, H.B., Cvijanovic, I.,  
377 Dahl-Jensen, D., Johnsen, S.J., Fischer, H., et al. A stratigraphic framework for abrupt climatic changes  
378 during the Last Glacial period based on three synchronized Greenland ice-core records: refining and  
379 extending the INTIMATE event stratigraphy. *Quat. Sci. Rev.* **2014**, *106*, 14-28.  
380 <http://dx.doi.org/10.1016/j.quascirev.2014.09.007>.
- 381 14. Lyakhovich, V.V. On pisolitic tufa on the Siberian platform. *Doklady AN SSSR* **1956**, *110*, 137-139. [In  
382 Russian].
- 383 15. Moore, J.Y., Peck, D.L. Accretionary lapilli in volcanic rocks of the Western Continental United States.  
384 *J. Geol.* **1962**, *70*, 182-194.
- 385 16. Kotova, L.N. Ash lapilli from Devonian volcanogenic-sedimentary series of Tarbagai Ridge. *Lithol.*  
386 *Mineral Resour.* **1966**, *2*, 58-64. [In Russian].
- 387 17. Shcherbakova, M.N. Ash rain in volcanogenic sediments of near-Balkhash (Kazakhstan). *Lithol.*  
388 *Mineral Resour.* **1972**, *1*, 155-160. [In Russian].

- 389 18. Dzozenidze, G.S., Markhinin, E.K. Volcanoclastic products and problem of their evolution. In  
390 *Problems of the volcanogenic-sedimentary lithogenesis*. Nauka Press: Moscow, Russia, 1974, pp. 4-12. [In  
391 Russian].
- 392 19. Mangerud, J., Lie, S.E., Furnes, H., Kristiansen, I.L., Lømo, L. A Younger Dryas Ash Bed in western  
393 Norway, and its possible correlations with tephra in cores from the Norwegian Sea and the North  
394 Atlantic. *Quat. Res.* **1984**, *21*, 85-104.
- 395 20. Kvamme, T., Mangerud, J., Furnes, H., Ruddiman, W.F. Geochemistry of Pleistocene ash zones in  
396 cores from the North Atlantic. *Norsk Geologisk Tidsskrift* **1989**, *69*, 251-272.
- 397 21. Ruddiman, W.F., Glover, L.K. Vertical mixing of ice-rafted volcanic ash in north Atlantic sediments.  
398 *Geol. Soc. Am. Bull.* **1972**, *83*, 2817-2836.
- 399 22. Bond, G.C., Mandeville, C., Hoffmann, S. Were rhyolitic glasses in the Vedde ash and in the North  
400 Atlantic's Ash Zone 1 produced by the same volcanic eruption? *Quat. Sci. Rev.* **2001**, *20*, 1189-1199.
- 401 23. Le Maitre, R.W., Bateman, P., Dudek, A., Keller, J., Lameyre, J., Le Bas, M.J., Sabine, P.A., Schmid, R.,  
402 Sorensen, H., Streickeisen, A., Woolley, A.R., Zanettin, B. *A Classification of Igneous Rocks and Glossary*  
403 *of Terms*. Blackwell Scientific Publications: Oxford, UK, 1989; 193 p.
- 404 24. Mutschler, F.E., Rougon, D.J., Lavin, O.P., Hughes, R.D. PETROS – A data bank of major element  
405 chemical analyses of igneous rocks for research and teaching (version 6.1). NOAA, National  
406 Geophysical and Solar-Terrestrial Data Center, Boulder, CO. 1981.
- 407 25. Wallrabe-Adams, H.J., Lackschewitz, K.S. Chemical composition, distribution, and origin of silicic  
408 volcanic ash layers in the Greenland – Iceland – Norwegian Sea: explosive volcanism from 10 to 300  
409 ka as recorded in deep-sea sediments. *Mar. Geol.* **2003**, *193*, 273-293.
- 410 26. Mortensen, A.K., Bigler, M., Grönvold, K., Steffensen, J.P., Johnsen, S.J. Volcanic ash layers from the  
411 Last Glacial Termination in NGRIP ice core. *J. Quat. Sci.* **2005**, *20*, 209-219.
- 412 27. Lacasse, C., Sigurdsson, H., Johanntson, H., Paterne, M., Carey, S. Source of Ash Zone 1 in North  
413 Atlantic. *Bull. Volcan.* **1995**, *57*, 18-32.